LETTERS
PUBLISHED ONLINE: 4 APRIL 2010 | DOI: 10.1038/NMAT2731
nature materials

Giant solid-state barocaloric effect in the Ni–Mn–In magnetic shape-memory alloy

Lluís Mañosa[1]*, David González-Alonso[1], Antoni Planes[1], Erell Bonnot[2], Maria Barrio[2], Josep-Lluís Tamarit[2], Seda Aksoy[3] and Mehmet Acet[3]

The search for materials showing large caloric effects close to room temperature has become a challenge in modern materials physics and it is expected that such a class of materials will provide a way to renew present cooling devices that are based on the vapour compression of hazardous gases. Up to now, the most promising materials are giant magnetocaloric materials. The discovery of materials showing a giant magnetocaloric effect at temperatures close to ambient has opened up the possibility of using them for refrigeration[1-3]. As caloric effects refer to the isothermal entropy change achieved by application of an external field, several caloric effects can take place on tuning different external parameters such as pressure and electric field. Indeed the occurrence of large electrocaloric[4,5] and elastocaloric[6] effects has recently been reported. Here we show that the application of a moderate hydrostatic pressure to a magnetic shape-memory alloy gives rise to a caloric effect with a magnitude that is comparable to the giant magnetocaloric effect reported in this class of materials. We anticipate that similar barocaloric effects will occur in many giant-magnetocaloric materials undergoing magnetostructural transitions involving a volume change.

The barocaloric effect refers to the isothermal entropy change or adiabatic temperature change on the application or withdrawal of an external pressure. This effect is used in most present cooling technologies that are based on the compression and expansion cycles of gases. On the other hand, barocaloric effects in the solid state have received little attention because the thermal effects were expected to be small. For example, the application of hydrostatic pressures of 5 kbar in a mixed crystalline compound ($Pr_{1-x}La_xNiO_3$) resulted in an effective cooling that was in competition with the elastic heating[7]. Application of uniaxial pressure slightly improved the measured values, but they were still close to those of elastic heating[8]. Here, we report a barocaloric effect of 24.4 $J\,kg^{-1}\,K^{-1}$ under a hydrostatic pressure of 2.6 kbar, at temperatures close to room temperature. This value is 20 times larger than the value resulting from elastic heating. Moreover, the magnitude found for the barocaloric effect compares well to the best values reported in giant magnetocaloric materials[9,10], which are nowadays being considered as alternatives for room-temperature refrigeration.

Giant caloric effects are expected to occur when a material undergoes a first-order phase transition. The possibility of inducing the transition by varying external fields such as magnetic, electric and stress gives rise to the reported giant magnetocaloric, electrocaloric and elastocaloric effects. Recently, it has been theoretically predicted[11,12] that some giant magnetocaloric materials would also show giant barocaloric effects. On the other hand, experiments have shown that hydrostatic pressure affects the magnetocaloric properties of several materials[13,14]. Here we directly measure the barocaloric effect resulting from the application of a hydrostatic pressure to a giant magnetocaloric material such as Ni–Mn–In.

Ni–Mn–Z (Z = Ga, In, Sn and Sb) alloys with compositions close to the stoichiometric Ni_2MnZ undergo a martensitic transformation from a high-temperature cubic (Heusler) structure to a close-packed martensitic phase[15] of lower crystallographic symmetry. In relation to the martensitic transition, several important functional properties such as inverse magnetocaloric effects[3], metamagnetic shape memory[16], magnetic superelasticity[17] and giant magnetoresistance[18] have been reported in this alloy family. We recently studied the influence of hydrostatic pressure on the magnetic and structural properties of Ni–Mn–In shape-memory alloys[19], and found that the properties of the martensitic transition were strongly affected by the application of hydrostatic pressure. This finding suggests that this material is a good candidate to show large barocaloric effects. As will be shown below, the physical origin of the large barocaloric effect found in this compound is the same as that reported for the inverse magetocaloric effect: the large entropy change accompanying the structural (martensitic) transition, which can be induced either by magnetic field or by hydrostatic pressure, or even by a combination of both (multicaloric effect). In magnetocaloric materials it has been pointed out that the entropy of a structural transition has a key role in the appearance of the giant magnetocaloric effect[20]. Our results suggest that such a situation should also hold for the appearance of other giant caloric effects.

In magnetic shape-memory alloys the martensitic transition temperature strongly depends on composition[15]. For the present study we selected a sample with a martensitic transition temperature close to room temperature, so that the desired caloric effect occurs in a temperature range useful for practical applications. Figure 1 shows low-field magnetization data recorded in zero-field-cooling, field-cooling and field-heating sequences. On cooling there is a sharp increase in magnetization at the ferromagnetic ordering temperature of the cubic phase, which is followed by a decrease at the martensitic transition. The small thermal hysteresis between field-cooling and field-heating sequences is associated with the first-order character of the martensitic transition, whereas the splitting between zero-field-cooling and field-cooling curves is indicative of the coexistence of antiferromagnetic and ferromagnetic exchange correlations in the martensitic state[21].

---

[1] Departament d'Estructura i Constituents de la Matèria, Facultat de Fısica, Universitat de Barcelona, Diagonal 647, Barcelona Knowledge Campus (BKC), 08028 Barcelona, Catalonia, [2] Departament de Física i Enginyeria Nuclear, ETSEIB, Universitat Politècnica de Catalunya, Diagonal 647 and Center for Research in NanoEngineering, Pascual i Vila, 15, Barcelona Knowledge Campus (BKC), 08028 Barcelona, Catalonia, [3] Experimentalphysik, Universität Duisburg-Essen, D-47048 Duisburg, Germany. *e-mail: lluis@ecm.ub.es.

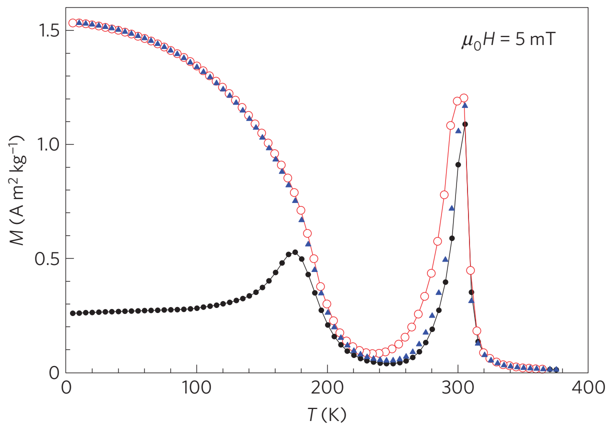

Figure 1 | Temperature dependence of the magnetization. Low-field magnetization as a function of temperature. Data are taken in the zero-field-cooling (filled circles), field-cooling (open circles) and field-heating (triangles) sequences.

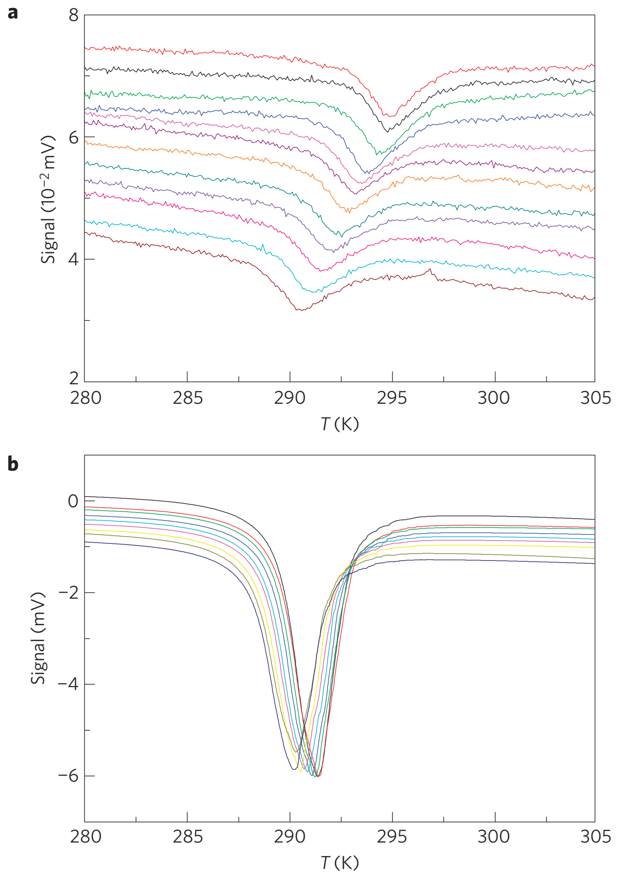

Figure 2 | Calorimetric signal as a function of temperature. **a**,**b**, Calorimetric curves at selected values of hydrostatic pressure (**a**) and magnetic field (**b**). The curves have been vertically displaced for clarity. From top to bottom the curves correspond to 2.6, 2.45, 2.3, 2.0, 1.8, 1.6, 1.4, 1.2, 1.0, 0.8, 0.4 and 0.2 kbar in **a** and 0, 0.19, 0.27, 0.36, 0.47, 0.59, 0.70, 0.87 and 0.94 T in **b**.

Caloric effects are usually quantified by isothermal entropy changes, which are computed using the Maxwell relations from measurements of an extensive quantity (magnetization, polarization and so on) while its conjugated thermodynamic generalized field (magnetic, electric and so on) is isothermally swept. In the study of the solid-state barocaloric effect this method is not readily feasible because the involved volume changes are small and they cannot be measured with the precision required to obtain reliable entropy data. The best-suited method is to directly measure the entropy change by a calorimetric technique. This technique has been shown to be very appropriate in the study of the magnetocaloric effect in giant magnetocaloric materials[22,23]. We have used a purpose-built calorimeter that operates under hydrostatic pressures up to 3 kbar. To study the magnetocaloric effect and relate the data to the barocaloric effect, we have used a second purpose-built calorimeter that operates under magnetic fields up to 1 T. Figure 2 shows the thermal curves as a function of temperature, obtained during cooling at selected values of the hydrostatic pressure (Fig. 2a) and magnetic field (Fig. 2b). A clear exothermal peak is observed corresponding to the latent heat of the martensitic transition. For conciseness, only results during cooling runs will be presented in this work. On heating, an endothermal peak is obtained at about 300 K (not shown here). From the calorimetric data, the entropy (S) change (referenced to a given state at T_0), is computed as[24]:

$$S(T,Y)-S(T_0,Y)=\int_{T_0}^{T}\frac{1}{T}\frac{\dot{Q}(Y)}{\dot{T}}\,\mathrm{d}T$$

where $\dot{Q}(Y)$ is the heat flux, $\dot{T}$ is the cooling rate and Y refers either to hydrostatic pressure p or to magnetic field H. The results obtained are shown in Fig. 3a,b ($T_0 = 300$ K). When the material undergoes the transition from the cubic to the martensitic phase, the entropy smoothly decreases down to a plateau close to -27 ± 3 J kg^{-1} K^{-1}. This value is the martensitic transition entropy change obtained by conventional differential scanning calorimetry at atmospheric pressure and in the absence of a magnetic field. There is a systematic shift of the entropy curves towards higher temperatures as the hydrostatic pressure increases, whereas they shift to lower temperatures with increasing magnetic field. Such a shift is more clearly seen in the insets of Fig. 3a and b, which show the temperature of the peak in the calorimetric curves (Fig. 2a and b) as a function of pressure and magnetic field, respectively. It is found that hydrostatic pressure stabilizes the martensitic phase whereas magnetic field stabilizes the cubic phase. From the insets in Fig. 3 we obtain the following changes in the transition temperature with pressure and field: $\mathrm{d}T/\mathrm{d}p = 1.8\pm0.2$ K kbar^{-1} and $\mathrm{d}T/\mathrm{d}(\mu_0H) = -1.4\pm0.2$ K T^{-1}.

The caloric effect at each temperature (ΔS) is calculated as the difference between the data at different pressure and magnetic-field values in Fig. 3a and b, respectively. Results are presented in Fig. 4a for the barocaloric effect and 4b for the magnetocaloric effect. It is worth noting that the isothermal application of pressure results in a decrease of entropy whereas application of a magnetic field results in an entropy increase. This result is consistent with the fact that pressure stabilizes the martensitic phase whereas magnetic field stabilizes the cubic phase. In spite of the small scatter of the data at low temperature, it is apparent that a large caloric effect is obtained in both cases. The values found for the entropy change compare well to those reported in other giant caloric materials such as giant magnetocaloric materials, electrocaloric and elastocaloric materials. On the other hand, it is important to note that the value found for the barocaloric effect at 2.6 kbar (24.4 J kg^{-1} K^{-1}) is about 20 times larger than the effect corresponding to elastic heating ($\simeq \beta v\Delta p = 1.2$ J kg^{-1} K^{-1}), where $\beta = 3.7\times10^{-5}$ K^{-1} is the thermal expansion and $v = 1.22\times10^{-4}$ m^3 kg^{-1} is the specific volume[25].

The peak values of ΔS in Fig. 4a,b, systematically increase (in absolute value) with increasing pressure and field. The maximum value for the external-field-induced entropy change would correspond to the transition entropy change (27 J kg^{-1} K^{-1}). The values achieved by moderate pressures of 2.6 kbar are already very close to the maximum attainable barocaloric effect. The temperature change associated with an adiabatic sweep of the

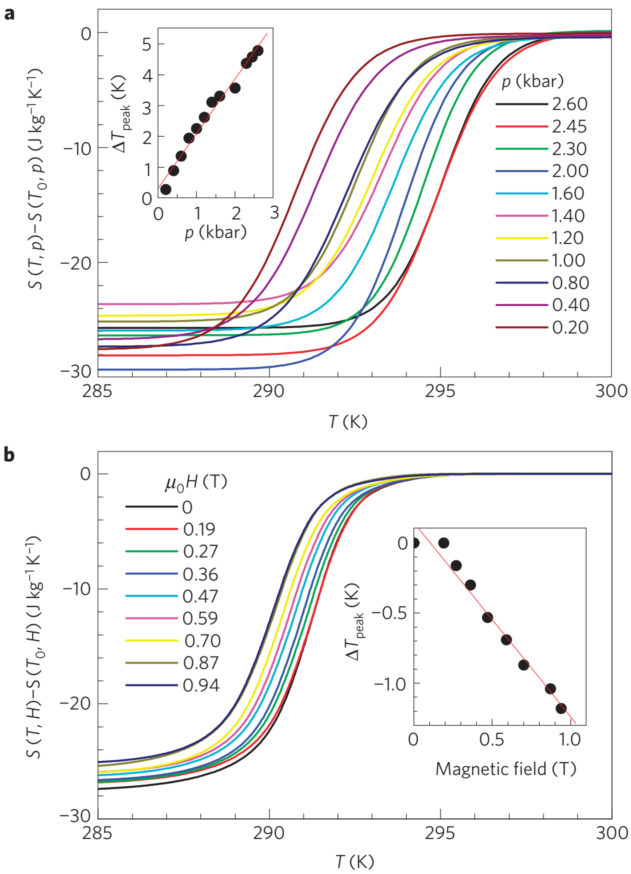

Figure 3 | Entropy as a function of temperature. a,**b**, Entropy values, referred to the value at ambient temperature, for selected values of hydrostatic pressure (**a**) and magnetic field (**b**). The insets show the shift in the temperature of the peak in the calorimetric curves as a function of hydrostatic pressure (**a**) and magnetic field (**b**).

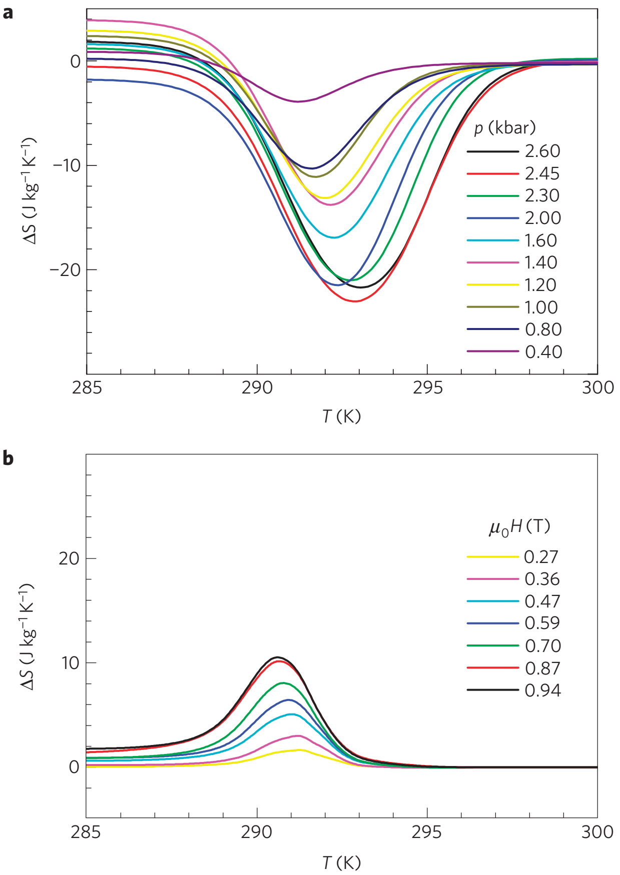

Figure 4 | Caloric effects in Ni–Mn–In. a,**b**, Barocaloric (**a**) and magnetocaloric (**b**) effects as a function of temperature, associated with the isothermal application of selected hydrostatic pressures (from $p = 0.2$ kbar up to the indicated value) and magnetic fields (from $H = 0$ up to the indicated value), respectively.

external field can be computed from the shift in the curves shown in Fig. 3. For a hydrostatic pressure of 2.6 kbar, $\Delta T \simeq 4.5$ K is obtained, and for a magnetic field of 0.94 T, $\Delta T \simeq 1.3$ K. These values are comparable to 6–7 K for the prototype giant magnetocaloric material Gd–Si–Ge (magnetic field of 2 T; ref. 9) or 12 K for the electrocaloric material $PbZr_{0.95}Ti_{0.05}O_3$ (electric field of 480 kV cm^{-1}; ref. 4). A significant figure of merit for cooling applications is the refrigerating cooling power ($RCP \simeq v^{-1}\Delta S \Delta T$), which is expressed in terms of energy per volume[9]. From the barocaloric data at 2.6 kbar, $RCP \simeq 1$ J cm^{-3}. It is worth noting that to achieve a similar RCP value, magnetic fields around 3.5 T would be required, which are not readily available with permanent magnets, whereas pressures up to 3 kbar are accessible by present technologies.

The large barocaloric effect found in Ni–Mn–In is a consequence of the volume and entropy discontinuities at a magnetostructural transition. This material also shows a large magnetocaloric effect. Actually, we can anticipate that large barocaloric effects will also be encountered in many giant magnetocaloric materials. In all of these materials, the large entropy content arises from magnetic first-order phase transitions. In magnetic systems showing time-reversal symmetry (which implies invariance under magnetization inversion) the first-order character of the transition requires a coupling to a secondary field[28], which is typically achieved through the coupling of magnetic exchange energy and interatomic distances. In the Ni–Mn–In alloy studied in this work, exchange interactions have been shown to be of Ruderman–Kittel–Kasuya–Yosida type[29,30], which are sensitive to changes in the atomic distances. In particular, the crystallographic symmetry reduction just below the martensitic transition is accompanied by a symmetry increase in the magnetic configuration. This is associated with an increase in the magnetic entropy, and can occur only in connection with the large volume decrease, which is responsible for the large barocaloric effect. Note also that the magnetic symmetry increase at the transition is at the origin of the inverse magnetocaloric effect shown by Ni–Mn–In. We anticipate that the reported barocaloric effect will inspire commercial applications for efficient and accurate solid-state refrigerating devices at ambient temperature. For instance, as both barocaloric and magnetocaloric effects occur in a single material, an accurate control of the temperature change could be achieved by fine tuning several external parameters. This advantage should result in more efficient and accurate cooling devices.

Methods

Ingots were prepared by arc melting the pure metals under argon atmosphere in a water-cooled copper crucible; the composition was determined by energy-dispersive X-ray photoluminescence analysis to correspond to $Ni_{49.26}Mn_{36.08}In_{14.66}$. The sample was encapsulated under argon in quartz glass and annealed at 1,273 K for two hours and subsequently quenched in an ice–water mixture. Magnetization measurements were carried out using a superconducting quantum interference device magnetometer. Calorimetric measurements were carried out using purpose-built calorimeters. Hydrostatic pressure calorimetry was carried out in a calorimeter similar to that described in ref. 26. The calorimetric block, made of a copper–beryllium alloy, is surrounded by an external heating and cooling vessel for temperature control. The temperature of the calorimeter is controlled by a Pt-100 thermometer embedded into the block. Samples were mixed with an inert perfluorinated liquid before they were hermetically sealed into Sn cells to ensure pressure transmission and to ascertain that in-cell volumes were free from residual air. Thermal sensors consist of type-K (chromel–alumel) thermocouples deeply inserted into the Sn sample and reference cells. The pressure into the calorimetric block was transmitted by compressing a cryogenic liquid and measured by calibrated Bourdon gauges with an accuracy better than 5 bar. Calorimetry under magnetic field was carried out in a calorimeter adapted from that described in ref. 27. The thermal sensors are batteries of thermocouples differentially connected. The sample is directly placed in contact with one of the sensors and a dummy sample is placed on the second sensor. The body of the calorimeter (copper block) is placed within the poles of an electromagnet, and is in thermal contact with a copper cylinder. The temperature of the calorimeter is controlled by a Pt-100 thermometer embedded into the block. A cryogenic fluid circulates through the copper cylinder and enables temperature control within the range 200–350 K. All heating and cooling runs were carried out at typical rates of about 1 K min^{-1}, and acquisition rates were 0.2 Hz and 0.5 Hz for the runs under pressure and magnetic field, respectively.

Received 18 December 2009; accepted 23 February 2010; published online 4 April 2010

References

1. Pecharsky, V. K. & Gschneidner, K. A. Jr Giant magnetocaloric effect in $Gd_5Si_2Ge_2$. *Phys. Rev. Lett.* **78,** 4494–4497 (1997).
2. Tegus, O., Brück, E., Buschow, K. H. J. & de Boer, F. R. Transition-metal-based magnetic refrigerants for room-temperature applications. *Nature* **415,** 150–152 (2002).
3. Krenke, T. *et al.* Inverse magnetocaloric effect in ferromagnetic Ni–Mn–Sn alloys. *Nature Mater.* **4,** 450–454 (2005).
4. Mischenko, A. S., Zhang, Q., Scott, J. F., Whatmore, R. W. & Mathur, N. D. Giant electrocaloric effect in thin-film $PbZr_{0.95}Ti_{0.05}O_3$. *Science* **311,** 1270–1271 (2006).
5. Neese, B. *et al.* Large electrocaloric effect in ferroelectric polymers near room temperature. *Science* **321,** 821–823 (2008).
6. Bonnot, E., Romero, R., Mañosa, L., Vives, E. & Planes, A. Elastocaloric effect associated with the martensitic transition in shape-memory alloys. *Phys. Rev. Lett.* **100,** 125901 (2008).
7. Müller, K. A. *et al.* Cooling by adiabatic pressure application in $Pr_{1-x}La_xNiO_3$. *Appl. Phys. Lett.* **73,** 1056–1058 (1998).
8. Strässle, Th., Furrer, A., Hossain, Z. & Geibel, Ch. Magnetic cooling by application of external pressure in rare-earth compounds. *Phys. Rev. B* **67,** 054407 (2003).
9. Gschneidner, K. A., Pecharsky, V. K. & Tsokol, A. O. Recent developments in magnetocaloric materials. *Rep. Prog. Phys.* **68,** 1479–1539 (2005).
10. Brück, E. Developments in magnetocaloric refrigeration. *J. Phys. D* **38,** R381–R391 (2005).
11. de Oliveira, N. A. Entropy change upon magnetic field and pressure variations. *Appl. Phys. Lett.* **90,** 052501 (2007).
12. de Medeiros, L. G., de Oliveira, N. A. & Troper, A. Barocaloric and magnetocaloric effects in $La(Fe_{0.89}Si_{0.11})_{13}$. *J. Appl. Phys.* **103,** 113909 (2008).
13. Morellon, L. *et al.* Pressure enhancement of the giant magnetocaloric effect in $Tb_5Si_2Ge_2$. *Phys. Rev. Lett.* **93,** 137201 (2004).
14. Lyubina, J., Nenkov, K., Schultz, L. & Gutfleisch, O. Multiple metamagnetic transitions in the magnetic refrigerant $La(Fe, Si)_{13}H_x$. *Phys. Rev. Lett.* **101,** 177203 (2008).
15. Planes, A., Mañosa, L. & Acet, M. Magnetocaloric effect and its relation to shape-memory properties in ferromagnetic Heusler alloys. *J. Phys. Condens. Matter* **21,** 233201 (2009).
16. Kainuma, R. *et al.* Magnetic-field-induced shape recovery by reverse phase transformation. *Nature* **439,** 957–960 (2006).
17. Krenke, T. *et al.* Magnetic superelasticity and inverse magnetocaloric effect in Ni–Mn–In. *Phys. Rev. B* **75,** 104414 (2007).
18. Sharma, V. K., Chattopadhyat, M. K., Shaeb, K. H. B., Chouhan, A. & Roy, S. B. Large magnetoresistance in $Ni_{50}Mn_{34}In_{16}$ alloy. *Appl. Phys. Lett.* **89,** 222509 (2006).
19. Mañosa, L. *et al.* Effects of hydrostatic pressure on the magnetism and martensitic transition of Ni–Mn–In magnetic superelastic alloys. *Appl. Phys. Lett.* **92,** 012515 (2008).
20. Pecharsky, V. K. & Gschneidner, K. A. Jr. in *Magnetism and Structure in Functional Materials* (eds Planes, A., Mañosa, L. & Saxena, A.) 199–222 (Springer Series in Materials Science, 2005).
21. Aksoy, S., Acet, M., Deen, P. P., Mañosa, L. & Planes, A. Magnetic correlations in martensitic Ni–Mn-based Heusler shape-memory alloys: Neutron polarization analysis. *Phys. Rev. B* **79,** 212401 (2009).
22. Casanova, F. *et al.* Direct observation of the magnetic-field-induced entropy change in $Gd_5(Si_xGe_{1-x})_4$ giant magnetocaloric alloys. *Appl. Phys. Lett.* **86,** 262504 (2005).
23. Mañosa, L., Planes, A. & Moya, X. Comment on 'The magnetocaloric effect of $LaFe_{11.6}Si_{1.4}$, $La_{0.8}Nd_{0.2}Fe_{11.5}Si_{1.5}$, and $Ni_{43}Mn_{46}Sn_{11}$ compounds in the vicinity of the first-order phase transition'. *Adv. Mater.* **21,** 3725–3726 (2009).
24. Planes, A. & Mañosa, L. Vibrational properties of shape memory alloys. *Solid State Phys.* **55,** 159–267 (2001).
25. Krenke, T. PhD thesis, Univ. Duisburg-Essen (2007).
26. Wurflinger, A. Differential thermal-analysis under high-pressure. 4. Low-temperature DTA of solid–solid and solid–liquid transitions of several hydrocarbons up to 3 kbar. *Ber. Bunsen Gesell. Phys. Chem. Chem. Phys.* **79,** 1195–1201 (1975).
27. Marcos, J. *et al.* A high-sensitivity differential scanning calorimeter with magnetic field for magnetostructural transitions. *Rev. Sci. Inst.* **74,** 4768–4771 (2003).
28. Tolédano, J. C. & Tolédano, P. *The Landau Theory of Phase Transitions* (World Scientific, 1987).
29. Sasioglu, E., Sandratskii, L. M. & Bruno, P. Role of conduction electrons in mediating exchange interactions in Mn-based Heusler alloys. *Phys. Rev. B* **77,** 064417 (2008).
30. Buchelnikov, V. D. *et al.* Monte Carlo study of the influence of antiferromagnetic exchange interactions on the phase transitions of ferromagnetic Ni-Mn-X alloys (X = In, Sn, Sb). *Phys. Rev. B* **78,** 184427 (2008).

Acknowledgements

This work was supported by CICyT (Spain), projects MAT2007-62100, and FIS2008-00837 and by Deutsche Forschungsgemeinschaft, grant No. SPP 1239. D.G. acknowledges support from DGICyT (Spain).

Author contributions

L.M. and A.P. planned the experiments in collaboration with J.T. and M.A. Sample preparation and magnetization measurements were carried out by S.A. and M.A. Calorimetric measurements under pressure were carried out by E.B. and M.B., and under magnetic field, by D.G. All authors discussed the results and analysed the data. The manuscript was prepared by L.M. in collaboration with A.P., J.T. and M.A.

Additional information

The authors declare no competing financial interests. Reprints and permissions information is available online at http://npg.nature.com/reprintsandpermissions. Correspondence and requests for materials should be addressed to L.M.